0026-895X/92/030569-08$03.00/0

MOLECULAR PHARMACOLOGY, 41:569-576

Molecular Conformation of Estramustine and Two Analogues

JOHN S. PUNZI, WILLIAM L. DUAX, PHYLLIS STRONG, JANE F. GRIFFIN, MARIA M. FLOCCO, DAVID E. ZACHARIAS, H. L. CARRELL, KENNETH D. TEW, and JENNY P. GLUSKER

Medical Foundation of Buffalo, Inc., Buffalo, New York 14203 (J.S.P., W.L.D., P.S., J.F.G.), and The Institute for Cancer Research, The Fox Chase Cancer Center, Philadelphia, Pennsylvania 19111 (M.M.F., D.E.Z., H.L.C., K.D.T., J.P.G.)

Received August 23, 1991; Accepted December 11, 1991

SUMMARY

The crystal and molecular structures of estramustine and two of its analogues have been determined by X-ray crystallographic techniques (a total of three different compounds). The compounds studied are estramustine [1,3,5(10)-estratriene-3,17β-diol-3-*N*,*N*-bis(2′-chloroethyl)carbamate] and its monohydrate, estromustine [17-oxo-1,3,5(10)-estratriene-3-yl-*N*,*N*-bis(2′-chloroethyl)carbamate], and 17-oxo-5-androsten-3β-yl-*N*,*N*-bis(2′-chloroethyl)carbamate. Three views of estramustine were obtained from the study of its two crystal forms. The main structural features found are as follows: (a) the geometries of the steroid moieties are closely similar to those of the parent steroids, (b) the bonds around the nitrogen atom of the nitrogen mustard grouping lie approximately in a plane in each structure, (c) the plane through the carbon atoms of the steroid A-ring lies approximately perpendicular to the plane through the carbamate atoms in each structure, (d) the carbonyl C-O of the carbamate points to the α side of the steroid moiety in each structure, and (e) one chlorine atom of the nitrogen mustard grouping makes a close contact [3.13 Å], in each structure, to the nitrogen atom. Hydrogen bonding to the carbamate appears to occur from the α side of the steroid; there is no hydrogen bonding to the nitrogen atom of the carbamate group. These structural data provide some steric explanations for the resistance of the carbamate to enzymatic hydrolysis. The long *in vivo* half-life of the intact estramustine molecule is a result of this stability. This is responsible for the absence of alkylating ability and the propensity of the drug to bind microtubule-associated proteins and express an antimitotic mechanism of action.

Estramustine phosphate (Estracyt; Emcyt) was first synthesized as a bis-2′-chloroethyl-substituted carbamate estradiol conjugate in the mid-1960s (1) and has been used ever since, with varying degrees of success, for the management of prostate cancer (2–4). The prevalence of serum phosphatases in the body ensures that the drug will be rapidly dephosphorylated in humans (5). Estramustine and its oxidized metabolite estromustine both possess long clinical half-lives (6), primarily because of the stability of the bond between the carbonyl carbon and the nitrogen of the mustard (7). Slow carbamate hydrolysis does result in low circulating levels of 17β-estradiol and estrone (2–4, 8); however, the pharmacological properties of estramustine have been found to be contingent upon the parent molecule and independent of the putative alkylating and steroidal activities (9). The release of a nitrogen mustard would require either esterase cleavage of the carbamate C-N bond followed by subsequent decarboxylation or a proteolytic event, but neither of these two activation steps has been demonstrated. Instead, the parent drug has been shown to bind MAPs (high molecular weight proteins that serve to stabilize microtubule networks in interphase cells and mitotic spindles in dividing cells), and this is the property primarily responsible for the cytotoxicity of estramustine and estromustine (9–12).

Accumulation of the drug in the prostate is effected by transient binding to the EMBP, which is evidenced in the ventral prostate of rats and humans (13–16). The dissociation constant (K_d) for estramustine binding to EMBP is in the nanomolar to micromolar range (17). This compares with a K_d value of 10–20 μM for the binding of the drug to target MAPs (10–13). Steroids such as testosterone or androstenedione have a low affinity for EMBP and do not bind to MAPs. Indeed, the interaction of estramustine with cellular protein targets does not appear to involve a steroid receptor (9). The reported vesicular uptake of estramustine in cultured human prostate cells, followed by the cytoskeletal and nuclear matrix binding (17), is a function of noncovalent drug-protein interactions (9).

It was considered that a comparison of the three-dimensional structures of estramustine and of some structurally related compounds may lead to an empirical model of the molecular basis for binding. Such a model might suggest which features of estramustine should be modified in order to develop new drugs with higher affinities for the target proteins. In order to obtain geometric data on low energy conformations of these flexible nitrogen mustard molecular structures, the following nitrogen mustard steroid derivatives (formulae in Fig. 1) have

This study was supported in part by Grant CN-10M from the American Cancer Society, Grants CA-10925, CA-06927, and DK-26546 from the National Institutes of Health, and an appropriation from the Commonwealth of Pennsylvania.

ABBREVIATIONS: MAP, microtubule-associated protein; EMBP, estramustine-binding protein.

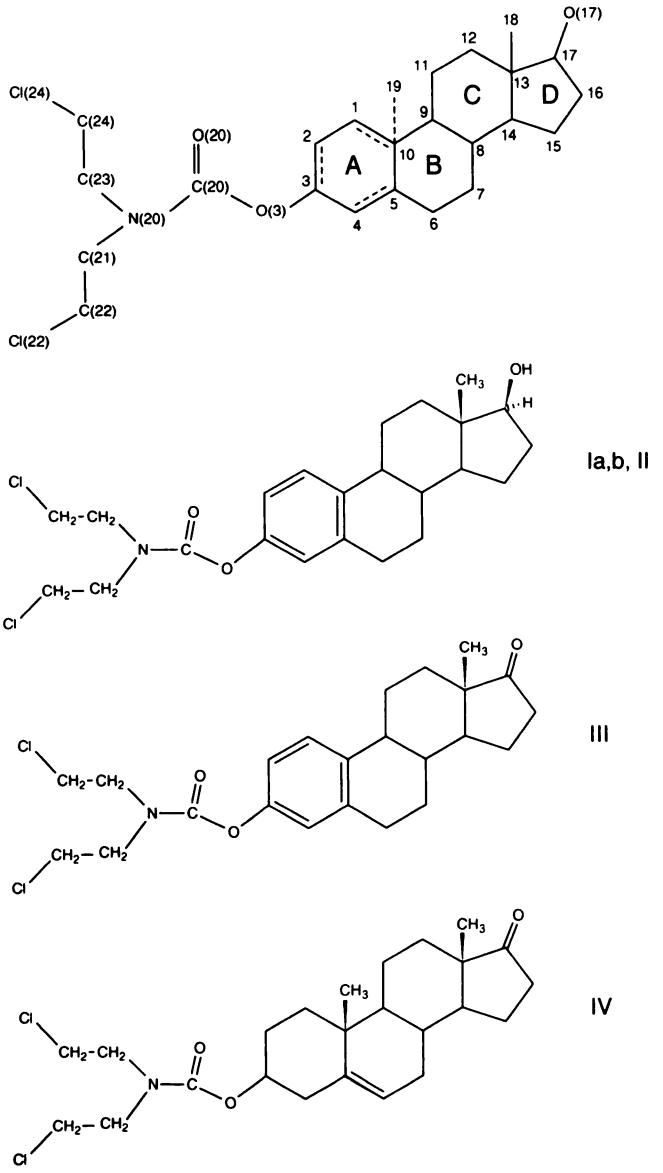

Fig. 1. Numbering system and structural formulae for the compounds for which crystal structure determinations were described in this study, **Ia, Ib, II** (estramustine), **III** (estromustine), and **IV**.

been determined by single-crystal X-ray diffraction: 1,3,5(10)-estratriene-3,17β-diol-3-*N*,*N*-bis(2′-chloroethyl)carbamate (estramustine) in an anhydrous form (I) and a hydrated form (II), 17-oxo-1,3,5(10)-estratriene-3-yl-*N*,*N*-bis(2′-chloroethyl) carbamate (estromustine) (III), and 17-oxo-5-androsten-3β-yl-*N*,*N*-bis(2′-chloroethyl)carbamate (IV). Relative binding affinities for the rat EMBP are in the ratios I and II, 1.00; III 1.16 and; IV, 0.23 (15).

Materials and Methods

Crystal data, data collection, and data refinement details are given in Table 1. In all cases the crystal structures were solved by use of direct methods, with the computer program MULTAN (18). Scattering factors were taken from *International Tables for X-Ray Crystallography* (19).

X-ray diffraction data (molybdenum radiation) for compound I were measured at a temperature of −120° on a Syntex/Nicolet/Siemens P3 diffractometer, with a variable ω-20 scan rate of 1.01–58.6°/min, and a 2θ range of 1.75–52°, to a maximum $\sin\theta/\lambda$ value of 0.617 Å^{-1}. This yielded 5082 unique Bragg reflections, of which 2656 were observed with $I \geq 2\sigma(I)$. These were corrected for Lorentz and polarization factors, and the absorption correction of Walker and Stuart (20) was applied. Full-matrix least-squares refinement of compound I was carried out with anisotropic thermal parameters for all 29 nonhydrogen atoms in one molecule and 23 nonhydrogen atoms in the other molecule (the molecule with disorder in the nitrogen mustard group). Isotropic thermal parameters were used for the remaining nonhydrogen atoms (in the nitrogen mustard group). The minimization function was $\sum[w(|F_o|-|F_c|)^2]$, where $w = 1/\sigma^2(F_o)$. All hydrogen atoms were placed at idealized positions by use of the computer program CALCAT (21) and by examination of the electron density map. The exceptions to this were H(O17) and H(O17)′; their positions were calculated based on the hydrogen bonds they form, as well as by an examination of the electron density map.

X-ray diffraction data for compound II (molybdenum radiation) were measured on a Syntex P3 diffractometer with a fixed scan, 3°/min scan rate, and 2θ range of 4–45°, to a maximum $\sin\theta/\lambda$ value of 0.538 Å^{-1}. This gave 2362 unique data, of which 1799 were observed with $F > 2\sigma(F)$. X-ray diffraction data (copper radiation) for III and IV were measured on an Enraf-Nonius CAD4 diffractometer with a variable (ω-2θ) scan, 5–75°/min scan rate, and 2θ range of 3–154°, to a maximum $\sin\theta/\lambda$ value of 0.632 Å^{-1}. Of 2660 and 2889 unique diffraction data, respectively, for III and IV, 2373 and 2592, respectively, were considered observed by the criterion $F > 2\sigma(F)$.

Lorentz and polarization corrections were applied, and normalized structure factors were calculated. Hydrogen atoms (nine for II, nine for III, and 25 for IV) were located from electron density difference maps after the heavier (i.e., nonhydrogen) atoms had been refined to convergence. Hydrogen atoms were placed in idealized positions (21) when well resolved electron density corresponding to hydrogen positions of reasonable geometry were not observed. Structures II, III, and IV were refined using a full-matrix least-squares technique for reflections with $F_{obs} > 2\sigma(F_{obs})$. Hydrogen atoms were refined isotropically and nonhydrogen atoms were refined anisotropically. Data reduction and statistical evaluation of diffraction data and other calculations for II, III, and IV were performed using standard computer programs (22, 23). Atomic positional and equivalent isotropic displacement parameters for the four structures are listed in Tables 2–5.[1]

Results

Four crystal structures, one of which contains two molecules in the asymmetric unit, are reported here. Two of these crystal structures are of estramustine itself, one a hydrated crystal and the other an anhydrous crystal; there are two molecules in the asymmetric unit of the anhydrous crystal. The nitrogen mustard group is disordered in one of the two molecules in the asymmetric unit of the anhydrous form. The other two crystal structures that we report here are of an estramustine analogue with the 17-hydroxyl group of estradiol converted to the carbonyl group of estrone (estromustine) and of an androgen analogue with a carbonyl group in the 17-position. The formulae of each are shown in Fig. 1. The observed conformations of the five crystallographically independent molecules are illustrated in stereodiagrams in Fig. 2. These stereodiagrams show the similarities in the overall shapes of the molecules, as well as differences in the nitrogen mustard conformations. The

[1] Additional data are available from NAPS (c/o Microfiche Publications, PO Box 3513, Grand Central Station, New York, NY 10163), (NAPS Document 04932).

TABLE 1
Crystallographic data for the nitrogen mustard steroids

	I	II	III	IV
Formula	$C_{23}H_{31}Cl_2NO_3$	$C_{23}H_{31}Cl_2NO_3 \cdot H_2O$	$C_{23}H_{29}Cl_2NO_3$	$C_{24}H_{35}Cl_2NO_3$
Formula weight	440.41	458.43	438.40	456.46
Growth conditions	Methyl *t*-butylether or 1:1 methanol/ methyl acetate	2:1 Acetone/H_2O	2:1 Ethanol/H_2O	2:1 Ethanol/H_2O
Crystal size (mm)	0.40 × 0.28 × 0.08	0.63 × 0.14 × 0.05	0.40 × 0.20 × 0.05	0.70 × 0.70 × 0.20
Crystal system	Orthorhombic	Orthorhombic	Orthohombic	Orthorhombic
Space group	$P2_12_12_1$	$P2_12_12_1$	$P2_12_12_1$	$P2_12_12_1$
Density (g/cm^3)	1.30	1.32	1.34	1.26
Unit cell data				
a (Å)	21.278 (5)	13.977 (9)	8.021 (1)	12.071 (2)
b (Å)	24.342 (5)	24.89 (1)	38.544 (5)	31.795 (6)
c (Å)	8.7215 (17)	6.645 (4)	7.021 (1)	6.294 (1)
Volume (Å^3)	4517	2312	2171	2415
Z	8	4	4	4
Diffractometer used	Syntex P3	Syntex P3	Enraf-Nonius CAD4	Enraf-Nonius CAD4
Radiation (λ, Å)	MoKα (0.71069)	MoKα (0.71069)	CuKα (1.54184)	CuKα (1.54184)
F(000)	1872	976	928	976
Unique data	K5082	2362	2600	2889
$I > 2\sigma(I)$[a]	2656			
$F > 2\sigma(F)$[a]		1799	2373	2592
R factor[b]	0.070	0.081	0.054	0.069
Weighted *R* factor[b]	0.063	0.107	0.062	0.079
Maximum residual density in final difference map (eÅ^{-3})	0.23	0.73	0.31	0.49
Maximum shift/error in refinement	0.44	0.06	0.05	0.08

[a] Data used in calculations.
[b] $R = \sum||Fo| - |Fc|| / \sum|Fo|$, weighted $R = [\sum w(|Fo| - |Fc|)^2 / \sum w(|Fo|)^2]^{1/2}$, where *w* is the weight of each observation and *Fo* and *Fc* are observed and calculated structure factors, respectively.

structures of **I**, **II**, and **III** have been superimposed in Fig. 3, which shows the results, in stereodiagrams, of superimposing the carbamate group (Fig. 3a) and ring C (Fig. 3b). These diagrams were the result of a least-squares fit (24). Because the molecules are composed of three parts, steroid, carbamate, and nitrogen mustard, these will be described separately.

Geometry of the steroid. The magnitudes of bond lengths and angles in the steroid rings are similar to those observed in the parent steroids (25–27). The fused ring system greatly limits the flexibility of the steroids. The principal source of molecular flexibility in estra-1,3,5(10)-triene structures lies in the B-ring, which normally ranges between an 8β-sofa and 7α,8β-half-chair conformation (25, 26). Examination of the asymmetry parameters (25), which are a quantitative measure of the deviation of the rings from the symmetric form, shows that the B-rings of the four crystallographically independent molecules of the estra-1,3,5(10)-triene derivatives (**Ia, Ib, II,** and **III**) each have a sofa conformation. The phenyl C(3)-O(3) distance varies from 1.41 to 1.44 Å and the ether oxygen angle C(3)-O(3)-C(20) from 116 to 118°. The *ipso* angle at substitution [C(2)-C(3)-C(4)] is 121–124°, except in **IV**, where it is 110.7° because the A-ring is saturated.

The observation that estramustine and estromustine have similar cytotoxic properties and bind to target proteins with about the same affinity suggests that both molecules adopt similar conformations. In order to examine the influence of the nitrogen mustard substituent on the conformation of the steroid nucleus, a least-squares fit of the corresponding atoms in **II** and the observed structure of estradiol hemihydrate (28) was performed using the software of the PROPHET system (29). The least-squares fit, illustrated in Fig. 4, demonstrates that the A-, B-, C-, and D-rings of estramustine are similar in conformation to those observed in estradiol. This implies that the carbamate and nitrogen mustard groups have had little effect on the conformation of the steroid. The fact that the androgen derivative exhibits a lower affinity for rat EMBP could be due to steric hindrance between the 19-methyl group and an amino acid side chain in the binding site or the phenolic ring forming a favorable interaction in the binding site. Because the compound exhibits a K_d in the nanomolar range and other steroids possessing 19-methyl groups (testosterone and androstenedione) exhibit K_d values in the micromolar range, the nitrogen mustard moiety must contribute significantly to the protein-ligand association.

Geometry of the nitrogen mustard group. Although the X-ray structure determinations demonstrate flexibility in the nitrogen mustard group, all of the structures show some common features. The average geometry of the mustard group in four observations, **Ia, II, III,** and **IV** (**Ib** is omitted because of disorder), is given in Fig. 5. Values are compared with those obtained from a search for the carbamate group in the Cambridge Structural Database (27). In all cases the bonds around the nitrogen atom lie in a plane. The torsion angles for this group are listed in Table 6. In four of the five crystallographically independent determinations (**Ia, II, III,** and **IV**), seven contiguous nonhydrogen atoms, C(3), O(3), C(20), O(20), N(20), C(21), and C(23), are coplanar with one another. The root mean square deviations from this plane and the angle between this plane and the plane of the A-ring in each steroid structure are listed in Table 7; the average angle is 78(6)°. In **Ib**, carbon atoms C(21) and C(23) are twisted out of the plane in opposite directions in the disordered fragments **Ib** and **Ib′**.

Perhaps the most significant feature of the observed conformations of the mustard groups is that in **Ia, II, III,** and **IV**

TABLE 2

Atomic coordinates for compound I: fractional positional parameters and equivalent isotropic atomic displacement parameters for nonhydrogen atoms, with estimated standard deviations in parentheses

Atom	Parameters			
	x/a(σ)	y/b(σ)	z/c(σ)	$U_{eq}(\sigma)^a$
		Å²		
Cl(22)	0.0584 (1)	−0.7490 (1)	−0.2391 (3)	0.138 (2)
Cl(24)	0.1959 (1)	−0.9707 (1)	−0.1027 (2)	0.092 (1)
O(3)	0.0118 (2)	−0.8792 (2)	−0.1203 (4)	0.069 (2)
O(17)	−0.4821 (2)	−0.9607 (2)	0.1004 (4)	0.073 (2)
O(20)	0.0408 (2)	−0.9357 (2)	−0.3124 (4)	0.067 (2)
N(20)	0.1092 (2)	−0.8748 (2)	−0.2084 (4)	0.054 (3)
C(1)	−0.1318 (2)	−0.9597 (2)	−0.0762 (6)	0.061 (3)
C(2)	−0.0695 (3)	−0.9465 (2)	−0.0742 (7)	0.067 (4)
C(3)	−0.0516 (2)	−0.8974 (2)	−0.1336 (7)	0.068 (4)
C(4)	−0.0931 (3)	−0.8612 (2)	−0.1953 (6)	0.062 (4)
C(5)	−0.1570 (2)	−0.8750 (2)	−0.1955 (6)	0.056 (3)
C(6)	−0.2018 (3)	−0.8327 (3)	−0.2617 (7)	0.079 (4)
C(7)	−0.2694 (2)	−0.8516 (2)	−0.2730 (6)	0.067 (4)
C(8)	−0.2868 (2)	−0.8865 (2)	−0.1347 (6)	0.049 (3)
C(9)	−0.2471 (2)	−0.9394 (2)	−0.1378 (6)	0.051 (3)
C(10)	−0.1773 (2)	−0.9245 (2)	−0.1374 (6)	0.056 (4)
C(11)	−0.2658 (2)	−0.9799 (2)	−0.0122 (7)	0.061 (4)
C(12)	−0.3374 (2)	−0.9912 (2)	−0.0065 (6)	0.058 (4)
C(13)	−0.3738 (2)	−0.9380 (2)	0.0052 (5)	0.046 (3)
C(14)	−0.3559 (2)	−0.9025 (2)	−0.1335 (6)	0.054 (3)
C(15)	−0.4044 (2)	−0.8563 (2)	−0.1368 (7)	0.063 (4)
C(16)	−0.4649 (2)	−0.8830 (2)	−0.0686 (7)	0.064 (7)
C(17)	−0.4447 (2)	−0.9424 (2)	−0.0257 (6)	0.055 (4)
C(18)	−0.3627 (3)	−0.9093 (2)	0.1580 (6)	0.060 (3)
C(20)	0.0534 (3)	−0.9003 (2)	−0.2237 (7)	0.058 (4)
C(21)	0.1233 (3)	−0.8317 (2)	−0.0982 (7)	0.075 (4)
C(22)	0.1301 (3)	−0.7752 (3)	−0.1687 (9)	0.096 (5)
C(23)	0.1609 (2)	−0.8928 (2)	−0.3080 (7)	0.064 (4)
C(24)	0.2153 (3)	−0.9170 (3)	−0.2278 (8)	0.085 (5)
O(3′)	−0.2417 (2)	−0.6149 (2)	−0.2362 (4)	0.072 (2)
O(17′)	−0.7130 (2)	−0.7918 (2)	−0.2751 (4)	0.076 (2)
O(20′)	−0.1998 (2)	−0.6323 (2)	−0.4703 (4)	0.083 (3)
N(20)′	−0.1409 (2)	−0.6015 (2)	−0.2734 (6)	0.091 (3)
C(1′)	−0.3718 (2)	−0.7054 (2)	−0.3490 (7)	0.065 (4)
C(2′)	−0.3106 (2)	−0.6881 (2)	−0.3173 (7)	0.068 (4)
C(3′)	−0.3025 (2)	−0.6343 (2)	−0.2831 (6)	0.057 (3)
C(4′)	−0.3501 (2)	−0.5972 (2)	−0.2729 (6)	0.056 (3)
C(5′)	−0.4117 (2)	−0.6151 (2)	−0.3038 (6)	0.055 (3)
C(6′)	−0.4641 (2)	−0.5735 (2)	−0.2843 (6)	0.063 (4)
C(7′)	−0.5291 (2)	−0.5944 (2)	−0.3363 (6)	0.057 (3)
C(8′)	−0.5376 (2)	−0.6545 (2)	−0.2872 (5)	0.046 (3)
C(9′)	−0.4900 (2)	−0.6905 (2)	−0.3736 (6)	0.051 (3)
C(10′)	−0.4225 (2)	−0.6697 (2)	−0.3403 (6)	0.051 (3)
C(11′)	−0.4988 (2)	−0.7513 (2)	−0.3359 (7)	0.063 (4)
C(12′)	−0.5661 (2)	−0.7716 (2)	−0.3670 (7)	0.063 (4)
C(13′)	−0.6134 (2)	−0.7363 (2)	−0.2789 (6)	0.048 (3)
C(14′)	−0.6033 (2)	−0.6761 (2)	−0.3266 (6)	0.047 (3)
C(15′)	−0.6622 (2)	−0.6470 (2)	−0.2643 (7)	0.065 (4)
C(16′)	−0.7144 (2)	−0.6914 (2)	−0.2744 (7)	0.070 (4)
C(17′)	−0.6819 (2)	−0.7430 (2)	−0.3316 (7)	0.058 (4)
C(18′)	−0.6080 (3)	−0.7459 (2)	−0.1057 (7)	0.076 (4)
C(20′)	−0.1948 (3)	−0.6175 (2)	−0.3394 (8)	0.065 (4)
Cl(22A)[b]	−0.1262 (1)	−0.5567 (1)	0.1687 (3)	0.078 (1)
Cl(22B)	−0.1235 (3)	−0.5755 (3)	0.1753 (8)	0.073 (2)
Cl(24A)	0.0120 (2)	−0.5806 (1)	−0.5324 (3)	0.091 (1)
Cl(24B)	0.0251 (2)	−0.6017 (2)	−0.4977 (5)	0.055 (1)
C(21A)	−0.1407 (4)	−0.5658 (4)	−0.1259 (11)	0.076 (3)
C(21B)	−0.1315 (7)	−0.6109 (6)	−0.1067 (18)	0.048 (4)
C(22A)	−0.1322 (5)	−0.6046 (4)	−0.0069 (14)	0.086 (3)
C(22B)	−0.1405 (8)	−0.5493 (7)	−0.0420 (20)	0.059 (5)
C(23A)	−0.0799 (4)	−0.6151 (4)	−0.3454 (11)	0.082 (3)
C(23B)	−0.0886 (7)	−0.5806 (7)	−0.3927 (20)	0.057 (5)
C(24A)	−0.0611 (5)	−0.5678 (4)	−0.4274 (13)	0.081 (4)
C(24B)	−0.0299 (8)	−0.6153 (7)	−0.3811 (19)	0.062 (5)

[a] $U_{eq} = (1/3)\sum_i\sum_j U_{ij}a_i^*a_j^*\cdot a_ia_j$.

[b] In this group of atoms, the A-atoms had fixed occupancies of 0.66 and the B-atoms, 0.34. The *U* values for these are U_{iso}.

TABLE 3

Atomic coordinates for compound II: fractional positional parameters and equivalent isotropic atomic displacement parameters for nonhydrogen atoms, with estimated standard deviations in parentheses

Atom	Parameters			
	x/a(σ)	y/b(σ)	z/c(σ)	$U_{eq}(\sigma)^a$
		Å²		
C(1)	0.0387 (7)	0.2661 (4)	0.0048 (16)	0.05 (1)
C(2)	0.0247 (7)	0.2967 (4)	−0.1573 (17)	0.05 (1)
C(3)	0.0958 (8)	0.3312 (4)	−0.2197 (15)	0.05 (1)
C(4)	0.1806 (7)	0.3333 (4)	−0.1232 (16)	0.04 (1)
C(5)	0.1948 (6)	0.3013 (3)	0.0491 (14)	0.03 (1)
C(6)	0.2910 (8)	0.3053 (4)	0.1591 (17)	0.05 (1)
C(7)	0.2903 (7)	0.2824 (3)	0.3638 (19)	0.06 (1)
C(8)	0.2402 (6)	0.2279 (3)	0.3623 (14)	0.04 (1)
C(9)	0.1349 (6)	0.2357 (3)	0.3153 (13)	0.03 (1)
C(10)	0.1244 (6)	0.2674 (3)	0.1213 (14)	0.03 (1)
C(11)	0.0800 (6)	0.1818 (4)	0.3121 (16)	0.05 (1)
C(12)	0.0947 (7)	0.1495 (4)	0.5069 (15)	0.05 (1)
C(13)	0.2012 (6)	0.1422 (3)	0.5533 (15)	0.04 (1)
C(14)	0.2472 (6)	0.1976 (3)	0.5671 (14)	0.04 (1)
C(15)	0.3437 (7)	0.1874 (4)	0.6526 (17)	0.06 (1)
C(16)	0.3269 (7)	0.1398 (4)	0.8045 (14)	0.04 (1)
C(17)	0.2238 (6)	0.1211 (3)	0.7620 (15)	0.04 (1)
C(18)	0.2482 (7)	0.1056 (3)	0.3993 (15)	0.05 (1)
C(20)	0.0345 (7)	0.4092 (4)	−0.3742 (15)	0.04 (1)
C(21)	0.0769 (8)	0.4188 (4)	−0.7376 (15)	0.05 (1)
C(22)	0.1675 (9)	0.4482 (4)	−0.7832 (17)	0.06 (1)
C(23)	−0.0266 (7)	0.4858 (3)	−0.5553 (15)	0.04 (1)
C(24)	0.0205 (8)	0.5344 (4)	−0.4540 (20)	0.07 (1)
Cl(22)	0.2570 (2)	0.4399 (1)	−0.5957 (7)	0.10 (1)
Cl(24)	0.0890 (3)	0.5741 (1)	−0.6141 (7)	0.10 (1)
N(20)	0.0329 (5)	0.4373 (3)	−0.5504 (11)	0.04 (1)
O(3)	0.0831 (4)	0.3622 (2)	−0.3953 (10)	0.05 (1)
O(17)	0.2097 (5)	0.0654 (2)	0.7879 (10)	0.05 (1)
O(20)	0.0005 (5)	0.4246 (3)	−0.2215 (10)	0.05 (1)
O(1W)	0.3513 (5)	0.0190 (2)	0.0301 (10)	0.06 (1)

[a] $U_{eq} = (1/3)\sum_i\sum_j U_{ij}a_i^*a_j^*\cdot a_ia_j$.

one chlorine atom makes a close contact of 3.11–3.24 Å with the nitrogen, as a result of two *gauche* twists in the chain connecting them. The Cl(22)-C(22)-C(21)-N(20) and Cl(24)-C(24)-C(23)-N(20) torsion angles may be either *gauche* (±60°) (**Ia, II, III,** and **IV**) or *trans* (180°) (**Ib, III,** and **IV**), as shown in Table 6. The *gauche* conformation brings the Cl(22) atom near O(3) and N(20), as shown in Table 8. In the four ordered structures, one chain of the nitrogen mustard has a *gauche* twist that folds a chlorine atom back towards the carbonyl group. The nonbonding distances between the Cl(22) and O(3) are compared in Table 8. The electronegative chlorine atom is probably seeking the electron-poor carbon of the carbonyl group. The second chloroethyl group is apparently flexible enough to be extended, as in **II** and **III**, or folded back, as in **Ia**. Certain features of the overall nitrogen mustard conformation are remarkably similar in all five observations (see Table 6), considering the fact that the number of possible conformations may be high. Because estramustine analogues with the chlorine replaced by hydroxyl are also active, analogous N···H-O interactions may occur. Thus, the chlorine is not critical to the bioactivity of the compound but may act to stabilize the linkage.[2] This characteristic folding pattern may be relevant to the stability of the carbonyl-nitrogen linkage and the concomitant lack of activation of the nitrogen mustard.

[2] B. Hartley-Asp, personal communication.

TABLE 4

Atomic coordinates for compound III: fractional positional parameters and equivalent isotropic atomic displacement parameters for nonhydrogen atoms, with estimated standard deviations in parentheses

Atom	Parameters			
	x/a(σ)	y/b(σ)	z/c(σ)	$U_{eq}(\sigma)^a$
			Å²	
C(1)	0.4772 (5)	0.3905 (1)	−0.3575 (6)	0.043 (1)
C(2)	0.5554 (6)	0.4024 (1)	−0.5210 (6)	0.046 (1)
C(3)	0.7074 (6)	0.3878 (1)	−0.5698 (6)	0.040 (1)
C(4)	0.7771 (5)	0.3618 (1)	−0.4664 (6)	0.039 (1)
C(5)	0.6993 (5)	0.3499 (1)	−0.3005 (6)	0.035 (1)
C(6)	0.7839 (5)	0.3212 (1)	−0.1893 (6)	0.043 (1)
C(7)	0.7220 (5)	0.3183 (1)	0.0157 (6)	0.036 (1)
C(8)	0.5306 (4)	0.3186 (1)	0.0175 (6)	0.031 (1)
C(9)	0.4680 (5)	0.3543 (1)	−0.0528 (6)	0.034 (1)
C(10)	0.5469 (5)	0.3646 (1)	−0.2425 (6)	0.034 (1)
C(11)	0.2748 (5)	0.3562 (1)	−0.0500 (6)	0.043 (1)
C(12)	0.2000 (5)	0.3465 (1)	0.1453 (7)	0.045 (1)
C(13)	0.2656 (5)	0.3109 (1)	0.2093 (6)	0.036 (1)
C(14)	0.4583 (5)	0.3122 (1)	0.2134 (6)	0.034 (1)
C(15)	0.5089 (5)	0.2802 (1)	0.3290 (6)	0.046 (1)
C(16)	0.3777 (6)	0.2800 (1)	0.4899 (7)	0.052 (1)
C(17)	0.2304 (6)	0.3001 (1)	0.4149 (6)	0.047 (1)
C(18)	0.1937 (6)	0.2815 (1)	0.0848 (8)	0.054 (1)
C(20)	0.9218 (6)	0.4202 (1)	−0.7160 (6)	0.041 (1)
C(21)	0.9052 (6)	0.4222 (1)	−1.0690 (6)	0.045 (1)
C(22)	0.8015 (7)	0.4504 (1)	−1.1546 (7)	0.063 (2)
C(23)	1.1318 (5)	0.4527 (1)	−0.8852 (6)	0.045 (1)
C(24)	1.0844 (6)	0.4900 (1)	−0.8561 (7)	0.056 (2)
Cl(22)	0.6395 (2)	0.4634 (1)	−0.9929 (3)	0.106 (1)
Cl(24)	1.2624 (2)	0.5174 (1)	−0.8738 (2)	0.075 (1)
N(20)	0.9830 (4)	0.4300 (1)	−0.8882 (5)	0.039 (1)
O(3)	0.7844 (4)	0.3992 (1)	−0.7389 (4)	0.046 (1)
O(17)	0.1038 (5)	0.3059 (1)	0.5026 (6)	0.076 (1)
O(20)	0.9764 (5)	0.4280 (1)	−0.5644 (4)	0.061 (1)

$^a U_{eq} = (1/3)\sum_i\sum_j U_{ij} a_i^* a_j^* \cdot a_i a_j$.

TABLE 5

Atomic coordinates for compound IV: fractional positional parameters and equivalent isotropic atomic displacement parameters for nonhydrogen atoms, with estimated standard deviations in parentheses

Atom	Parameters			
	x/a(σ)	y/b(σ)	z/c(σ)	$U_{eq}(\sigma)^a$
			Å²	
C(1)	0.4591 (4)	0.4881 (1)	0.2173 (7)	0.057 (1)
C(2)	0.4355 (4)	0.4427 (1)	0.1610 (7)	0.066 (2)
C(3)	0.5215 (4)	0.4144 (1)	0.2607 (8)	0.059 (1)
C(4)	0.5219 (4)	0.4194 (1)	0.5006 (7)	0.054 (1)
C(5)	0.5444 (3)	0.4649 (1)	0.5580 (6)	0.044 (1)
C(6)	0.6270 (3)	0.4747 (1)	0.6915 (7)	0.047 (1)
C(7)	0.6557 (3)	0.5182 (1)	0.7559 (7)	0.048 (1)
C(8)	0.5641 (3)	0.5498 (1)	0.7096 (6)	0.042 (1)
C(9)	0.5178 (3)	0.5427 (1)	0.4845 (6)	0.044 (1)
C(10)	0.4685 (3)	0.4977 (1)	0.4579 (6)	0.042 (1)
C(11)	0.4389 (4)	0.5781 (1)	0.4143 (7)	0.060 (1)
C(12)	0.4831 (5)	0.6224 (1)	0.4459 (8)	0.066 (2)
C(13)	0.5196 (4)	0.6284 (1)	0.6768 (7)	0.055 (1)
C(14)	0.6063 (3)	0.5946 (1)	0.7279 (7)	0.048 (1)
C(15)	0.6582 (4)	0.6095 (1)	0.9387 (8)	0.062 (1)
C(16)	0.6640 (5)	0.6576 (1)	0.9073 (10)	0.078 (2)
C(17)	0.5844 (5)	0.6674 (1)	0.7283 (9)	0.072 (2)
C(18)	0.4190 (4)	0.6280 (1)	0.8303 (8)	0.068 (2)
C(19)	0.3530 (3)	0.4940 (1)	0.5627 (8)	0.058 (1)
C(20)	0.5583 (4)	0.3514 (1)	0.0703 (9)	0.068 (2)
C(21)	0.4099 (6)	0.2977 (2)	0.0971 (11)	0.092 (2)
C(22)	0.3158 (6)	0.2979 (3)	−0.0834 (19)	0.142 (4)
C(23)	0.5876 (6)	0.2839 (2)	−0.1008 (14)	0.101 (3)
C(24)	0.5701 (7)	0.2890 (2)	−0.3247 (14)	0.111 (3)
Cl(22)	0.3076 (2)	0.3428 (1)	−0.2183 (6)	0.155 (1)
Cl(24)	0.6534 (2)	0.2504 (1)	−0.4686 (4)	0.142 (1)
N(20)	0.5183 (4)	0.3127 (1)	0.0237 (8)	0.075 (2)
O(3)	0.4963 (3)	0.3710 (1)	0.2126 (6)	0.073 (1)
O(17)	0.5768 (4)	0.7013 (1)	0.6385 (8)	0.111 (2)
O(20)	0.6426 (3)	0.3657 (1)	−0.0084 (7)	0.087 (1)

$^a U_{eq} = (1/3)\sum_i\sum_j U_{ij} a_i^* a_j^* \cdot a_i a_j$.

A search of the Cambridge Structural Database (27) showed that chlorambucil (30), which is clinically active as a nitrogen mustard, contains the same mustard grouping. This compound also contains a phenyl group attached to the nitrogen of the mustard group, so that in both estramustine and chlorambucil the nitrogen is attached to an sp^2 carbon atom. However, each N-CH_2-CH_2-Cl group is extended (*trans*). In chlorambucil the nitrogen mustard has alkylating activity, presumably because an aziridine ring can be formed. In estramustine, on the other hand, the presence of a carbonyl group adjacent to the nitrogen mustard results in the nitrogen atom being part of an amide group (rather than an aromatic amine, as in chlorambucil). Therefore, an aziridine ring will probably not be formed in estramustine, because the carbonyl oxygen rather than the nitrogen would attract the -CH_2-CH_2^+ group [C(21)-C(22) or C(23)-C(24)] if the chloride was a leaving group.

Geometry of the carbamate group. The planar carbamate group contains three eclipsed 1,4 interactions. The C(3)-O(3)-C(20) = O(20) group is *cis* (average torsion angle, 2°) (Table 6) in each case. The *cis* relation of one O(20) = C(20)-N(20)-C(23) group with an average nonbonded distance between O(20)···C(23) of 2.74(2) Å opens the O(20)-C(20)-N(20) angle to 124.1(6)°. The C(20)-N(20)-C(21) angle opens up to 123.9(6)°, with an O(3)···C(21) nonbonded distance of 2.66(1) Å. The C(20)-N(20) distance in the carbamate O(20) = C(20)-N(20) group is considerably shorter (1.35 Å) than that of the C(21 or 23)-N(20) distances involving the chloromethyl groups (1.45–1.45 Å). This indicates some double-bond character to this bond, as in peptide groups (31), which may account for the planarity of the carbamate group. Average distances and angles from this study are compared, in Fig. 5, with those from the Cambridge Structural Database. The agreement is within expected errors.

The phenyl -O(3)-C(3) torsion angles vary from 65° and 84° for **I** and **II** to 106–107° for **III** and **IV**. If the four molecules are docked on top of each other via the carbamate N(20)-C(20)-O(20)-O(3) group, then C(3) of the steroid and the first carbon in each -CH_2-CH_2Cl group lie in that same plane. The steroid lies with its ring system in a plane roughly perpendicular to that of the carbamate groups, with the methyl groups on the β side pointing away from the direction of the carbamate carbonyl group.

Slight variation is seen in the orientation of the steroid ring system with respect to the carbamate group. The carbamate group forms a hydrogen bond to O(17) of another molecule (**Ia** and **Ib**) or a water molecule (**II**) (see Table 9). There is no water or hydroxyl to form this bond in molecules **III** or **IV**.

Discussion

Conjugates of steroids and nitrogen mustards are generally designed to deliver the cytotoxic alkylating function to a tumor cell population that expresses significant levels of the particular

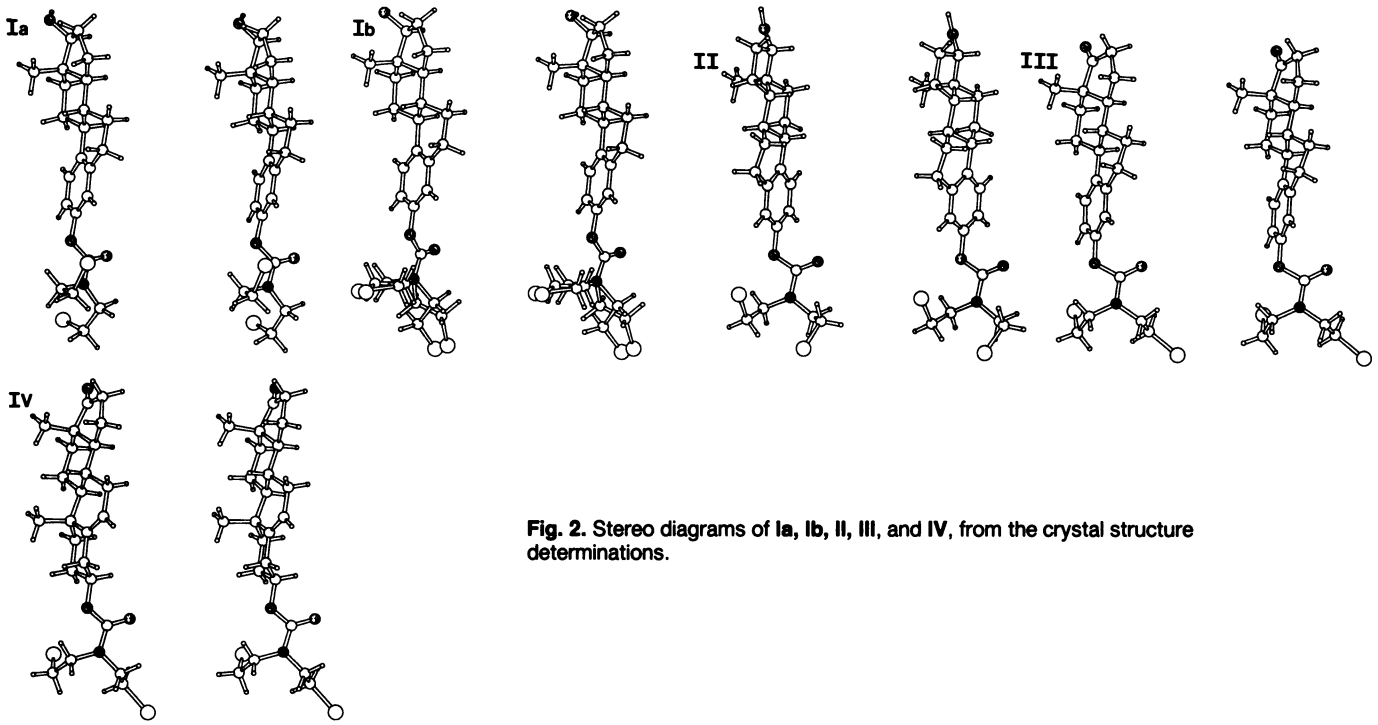

Fig. 2. Stereo diagrams of **Ia, Ib, II, III**, and **IV**, from the crystal structure determinations.

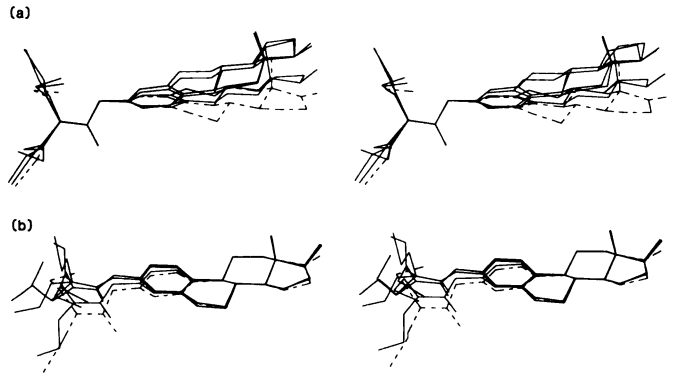

Fig. 3. Stereo diagrams of least-squares fits of the carbamate group (a) and the C-rings of **Ia, Ib, II** (——) and **III** (– – –) (b). In a (*right*), the upper molecules are **Ia** and **Ib** and the central molecule is **II**.

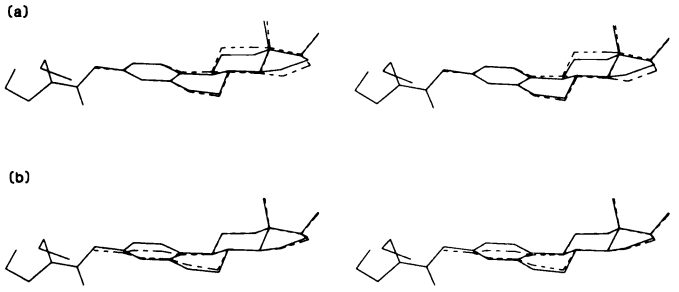

Fig. 4. Stereo diagram of a least-squares fit of ring A (a) and ring C (b) for **Ia** (——) and estradiol hemihydrate (28) (– – –).

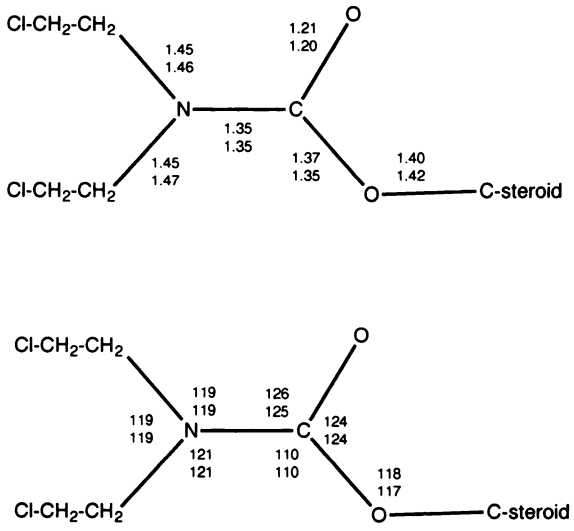

Fig. 5. Average geometry of carbamate group in **Ia, II, III**, and **IV** (*lower values*), compared with values obtained by a search of the Cambridge Structural Database (27) (*upper values*).

steroid receptor. This achieves a preferential delivery and incorporation of the active drug species. Drugs such as prednimustine (prednisolone ester of chlorambucil) exemplify this design. Unlike estramustine, prednimustine has an ester linkage, which is readily hydrolyzed by serum esterases. The presence of the carbamate in estramustine significantly changes the properties of the drug, creating a biological half-life in humans of >16 hr (6). In so doing, this stabilization has produced a drug with an unpredicted and unexpected antimicrotubule mechanism of action. An overview of the structures of many antimitotic drugs shows that an aminocarboxyalkyl group occurs in many of them. By a series of chemical substitution studies, Gupta (32) was able to show that the antimicro-

TABLE 6

Torsion angles for the nitrogen mustard group in compounds I–IV

	Torsion angles					
	Ia	Ib(A)[a]	Ib(B)[a]	II	III	IV
C(3)-O(3)-C(20)-N(20)	172.9°	−175.6°	−175.6°	175.5°	−178.9°	−173.2°
C(3)-O(3)-C(20)-O(20)	−6.9°	3.7°	3.7°	−2.3°	1.6°	7.9°
O(3)-C(20)-N(20)-C(21)	0.5°	−20.8°	30.1°	0.6°	5.6°	9.2°
·····C(23)	178.6°	−162.6°	−157.7°	173.0°	−179.9°	−169.0°
C(20)-N(20)-C(21)-C(22)	−107.8°	97.5°	−105.5°	−105.2°	98.3°	103.6°
····C(23)-C(24)	−116.3°	98.3°	−120.2°	78.9°	−82.5°	−88.9°
N(20)-C(21)-C(22)-Cl(22)	68.7°	176.0°	−178.8°	61.0°	−57.0°	−48.6°
···C(23)-C(24)-Cl(24)	52.9°	−176.6°	177.0°	90.3°	−174.9°	−177.1°

[a] Disordered nitrogen mustard group indicated by Ib(A) and Ib(B).

TABLE 7

Angle between the plane of C(3), O(3), C(20), O(20), N(20), C(21), and C(23) and the plane of the A-ring, together with root mean square deviations from the plane

	Angle between planes	Root mean square deviation
		Å
Ia	73.2°	0.04
Ib	53.8°	0.17
II	78.7°	0.04
III	72.5°	0.02
IV	86.7°	0.08

TABLE 8

Intramolecular nonbonding distances between chlorine atoms of the nitrogen mustard group, O(3), and N(20)

	Intramolecular distances				
	Cl(22)···Cl(24)	Cl(22)···O(3)	Cl(24)···O(3)	Cl(22)···N(20)	Cl(24)···N(20)
			Å		
Ia	6.25	3.48 (*g*)[a]	4.51 (*g*)	3.26 (*g*)	3.12 (*g*)
Ib(A)[b]	6.81	4.53 (*t*)	6.04 (*t*)	4.02 (*t*)	3.99 (*t*)
Ib(B)[b]	6.70	4.49 (*t*)	6.13 (*t*)	3.98 (*t*)	4.04 (*t*)
II	4.09	3.38 (*g*)	5.47 (*g*)	3.15 (*g*)	3.52 (*g*)
III	5.48	3.26 (*g*)	6.03 (*t*)	3.13 (*g*)	4.05 (*t*)
IV	5.34	3.64 (*g*)	6.06 (*t*)	3.11 (*g*)	4.02 (*t*)

[a] *g*, *gauche*; *t*, *trans* for the N-C-C-Cl torsion angle (see Table 6).
[b] Disordered structure.

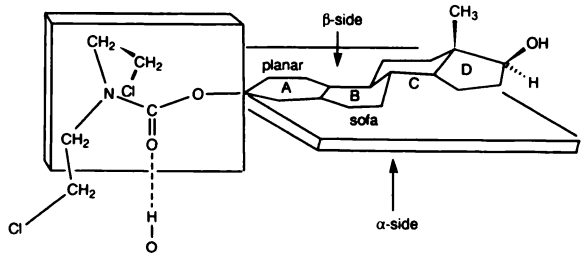

Fig. 6. Diagram of features of the molecular structure of estramustine, showing intermolecular interactions that may be significant in its binding *in vivo*.

tubule properties of nocodazole and other benzimidazole carbamates were diminished or abolished if the aminocarboxyalkyl group was altered. Many other antimicrotubule agents have this motif in their structure, including the simplest, isopropyl-*N*-phenylcarbamate. Furthermore, virtually all antimicrotubule drugs have aliphatic or aromatic ring substituents of varying degrees of complexity (33), indicating that binding avidity may be determined not only by hydrogen bonding but also by hydrophobic interactions. These properties would be consistent with the noncovalent reversible effects of estramustine on the cytoskeletons of cells in culture (9). Substituents that alter the planarity and/or hydrophobicity of the ring structures can influence the binding constant of the drug for the target protein. The steroid ring of estramustine provides the hydrophobicity that contributes to overall binding avidity. The antimitotic properties of diethylstilbesterol (34), although certainly not the primary pharmacological property of this agent, also indicate the possible role of the planar hydrophobic steroid nucleus in determining binding to microtubule structures.

With these structure-activity relationships in mind, crystal and molecular structures have been determined for three compounds (five independent observations) in which a nitrogen mustard is linked to a steroid nucleus by a carbamate bridge. The nitrogen mustard substituent had little effect on the overall conformation of the steroid nucleus. Only three conformations were observed for the nitrogen mustard side chains; they were characterized by close Cl-Cl and Cl-N contacts, suggesting energetically favorable interactions between these atoms in these structures. This favorable Cl-N interaction may be important for the inherent stability of the parent drug. It is possible that the electronegativity of the Cl has an impact on the accessibility of the carbamate-ester linkage to hydrolytic enzymes.

The structural information obtained from this investigation, diagrammed in Fig. 6, indicates that the carbamate group, all carbon atoms bonded directly to nitrogen of the mustard group, and C(3) of the steroid lie in a plane. The steroid ring system in each case is approximately perpendicular to this carbamate plane. The carbonyl group of the carbamate group points to the α side of the steroid. Because this carbamate group has converted the mustard nitrogen atom from an amine to an amide, it is not surprising that the compound does not behave as an alkylating agent. There is a weak interaction between one CH_2-CH_2-Cl group and the nitrogen and/or carbonyl group, possibly resulting from the charge distributions in the two groups.

The carbamate group, with a short C-N bond analogous to that in peptides, is planar and unlikely to form an aziridine ring. This may explain the lack of alkylating activity in estramustine. It is interesting, in this context, to note that many of the antimitotic agents that are natural products (e.g.,dolastatin

TABLE 9

Hydrogen bonding in estramustine crystals

Diagram is in deposited material.

	H bond donor	H bond acceptor	O····O distance	O····O distance
			Å	Å
Ia	O17-HO17·····O20	$-½ - x, -2-y, z + ½$	2.915	1.95
Ib	O17′-HO17·····O20′	$x - ½, -1½ - y, -z - 1$	2.902	1.90
II	O17-H17B·····O1W	$x, y, 1 + z$	2.800	1.75
	O1W-H1W·····O17B	$½ + x, -y, z - ½$	2.841	1.82
	O1W[a] ·····O19	$½ + x, ½ - y, -z$	2.819	

[a] Hydrogen atom not located.

10) (35) are short peptides and thereby show similarities to the carbamate bonding in estramustine.

The geometry of intermolecular interactions appears consistent for all five structures studied, in that the carbamate carbonyl group forms a hydrogen bond to the α side of the molecule. The nitrogen atom of the carbamate group is not involved in hydrogen bonding. This provides a model, shown in Fig. 6, for the molecular basis of the binding of estramustine to its intracellular targets. The structural characterization of the estramustine molecules has offered insight into those features of the drug responsible for its noncovalent binding to MAPs. It should be possible to extrapolate the present findings to other steroid-alkylating agent complexes and to other antimitotic drugs that have an aminocarboxyalkyl group as an integral part of their structure.

Acknowledgments

We thank Drs. R. Piccolini and B. Hartley-Asp for helpful discussions. The authors thank the AB Leo Company, Helsingborg, Sweden, for providing samples of the nitrogen mustard steroids.

References

1. Fex, H. J., K. B. Hogberg, I. Konyves, and P. H. O. J. Kneip. Certain steroid *N*-bis-(halo-ethyl)-carbamates. United States Patent No. 3 299 104, 17.1 (1967).
2. Jönsson, G., B. Högberg, and T. Nilson. Treatment of advanced prostatic carcinoma with estramustine phosphate. *Scand. J. Urol. Nephrol.* **11**:231–238 (1977).
3. Hedlund, P. O. Estracyt—mode of action and clinical experience. *Prog. Clin. Biol. Res.* **243B:** 215–219 (1987).
4. Murphy, G. P. *A Current Review of the Clinical Experience with Estracyt.* Alan R. Liss, Inc., New York, 221–225 (1987).
5. Tritsch, G. L., S.K. Shukla, A. Mittelman, and G. P. Murphy. Estracyt as a substrate for phosphatase in human serum. *Invest. Urol.* **12**:38–39 (1974).
6. Gunnarsson, P. O., and G. P. Forshell. Clinical pharmacokinetics of estramustine phosphate. *Urology* **23**:22–27 (1984).
7. Verbiscar, A. J., and L. G. Abood. Carbamate ester latentiation of physiologically active amines. *J. Med. Chem.* **13**:1176–1179 (1970).
8. Forshell, G. P., J. Muntzing, A. Ek, E. Lindstedt, and H. Dencker. The absorption, metabolism and excretion of estracyt in patients with prostate cancer. *Invest. Urol.* **14**:128–131 (1976).
9. Tew, K. D., and B. Hartley-Asp. Cytotoxic properties of estramustine unrelated to alkylating and steroid constituents. *Urology* **23**:28–33 (1984).
10. Stearns, M. E., and K. D. Tew. Anti-microtubule effects of estramustine, an antiprostatic tumor drug. *Cancer Res.* **45**:3891–3897 (1985).
11. Stearns, M. E., and K. D. Tew. Estramustine binds MAP-2 to inhibit microtubule assembly *in vitro*. *J. Cell Sci.* **89**:331–342 (1988).
12. Stearns, M., M. Wang, K. D. Tew, and L. I. Binder. Estramustine binds a MAP-1-like protein to inhibit microtubule assembly *in vitro* and disrupt microtubule organization in DU 145 cells. *J. Cell Biol.* **107**:2647–2656 (1988).
13. Heyns, W., B. Peeters, J. Mous, W. Rombauts, and P. De Moor. Purification and characterization of prostatic binding protein and its subunits. *Eur. J. Biochem.* **89**:181–186 (1978).
14. Forsgren, B., and P. Björk. Specific binding of estramustine to prostatic proteins. *Urology* **23**:34–38 (1984).
15. Forsgren, B., J.-A. Gustafsson, A. Pousette, and B. Högberg. Binding characteristics of a major protein in rat ventral prostate cytosol that interacts with estramustine, a nitrogen mustard derivative of 17β-estradiol. *Cancer Res.* **39**:5155–5164 (1979).
16. Björk, P., B. Forsgren, J.-A. Gustafsson, A. Pousette, and B. Högberg. Partial characterization and "quantitation" of a human prostatic estramustine-binding protein. *Cancer Res.* **42**:1935–1942 (1982).
17. Stearns, M. E., D. P. Jenkins, and K. D. Tew. Dansylated estramustine, a fluorescent probe for studies of uptake and identification of intracellular targets. *Proc. Natl. Acad. Sci. USA* **82**:8483–8487 (1985).
18. Main, P., L. Lessinger, M. M. Woolfson, G. Germain, and J. P. Declercq. MULTAN 77: a system of computer programs for the automatic solution of crystal structures from X-ray diffraction data. Universities of York, England, and Louvain, Belgium (1977).
19. *International Tables for X-ray Crystallography*, Vol. IV. Kynoch Press, Birmingham, UK (1974).
20. Walker, N., and D. Stuart. An empirical method for correcting diffractometer data for absorption effects. *Acta Crystallogr. A* **39**:158–166 (1983).
21. Carrell, H.L., H.-S. Shieh, and F. Takusagawa. CALCAT: program for calculation of idealized atomic positions. The Crystallographic Program Library of the Institute for Cancer Research, Fox Chase Cancer Center, Philadelphia, PA, (1981).
22. Blessing, R. H. Data reduction and error analysis for accurate single crystal diffraction intensities. *Crystallogr. Rev.* **1**:3–58 (1987).
23. Stewart, J. M., ed. *The X-ray System Technical Report* TR-446. Computer Science Center, University of Maryland, College Park, MD (1976).
24. Carrell, H. L. MOLDOCK. Institute for Cancer Research, The Fox Chase Cancer Center, Philadelphia, PA (1991).
25. Duax, W. L., and D. A. Norton, eds. *Atlas of Steroid Structure*, Vol. 1. Plenum, New York (1975).
26. Griffin, J. F., W. L. Duax, and C. M. Weeks, eds. *Atlas of Steroid Structure*, Vol. 2 Plenum, New York (1984).
27. Allen, F. H., S. Bellard, M. D. Brice, B. A. Cartwright, A. Doubleday, H. Higgs, T. Hummelink, B. G. Hummelink-Peters, O. Kennard, W. D. S. Motherwell, J. R. Rodgers, and D. G. Watson. The Cambridge Crystallographic Data Centre: computer-based search, retrieval, analysis and display of information. *Acta Crystallogr. B* **35**:2331–2339 (1979).
28. Busetta, B., and M. Hospital. Structure cristalline et moleculaire de l'oestradiol hemihydrate. *Acta Crystallogr. B* **28**:560–567 (1972).
29. PROPHET. National Institutes of Health, Bethesda, MD.
30. Ollis, J., and V. J. James. *p*-(Di-2-chloroethyl)aminophenylbutyric acid, chlorambucil-$C_{14}H_{19}Cl_2NO_2$. *Cryst. Struct. Commun.* **4**:413–416 (1975).
31. Marsh, R. E., and J. Donohue. Crystal structure studies of amino acids and peptides. *Adv. Protein Chem.* **22**:235–256 (1967).
32. Gupta, R. S. Cross-resistance of nocodazole-resistant mutants of CHO cells toward other microtubule inhibitors: similar mode of action of benzimidazole carbamate derivatives and NSC 181928 and TN-16. *Mol. Pharmacol.* **30**;142–148 (1986).
33. Tew, K. D., and M. E. Stearns. Estramustine: a nitrogen mustard/steroid with antimicrotubule activity. *Pharmacol. Ther.* **43**:299–319 (1989).
34. Parry, E. M., N. Danford, and J. M. Pary. Differential staining of chromosomes and spindle and its use as an assay for determining the effects of diethylstilbesterol on cultured mammalian cells. *Mutat. Res.* **105**:243–252 (1982).
35. Bai, R., G. R. Pettit, and E. Hamel. Binding of dolastatin 10 to tubulin at a distinct site for peptide antimitotic agents near the exchangeable nucleotide and *Vinca* alkaloid sites. *J. Biol. Chem.* **265**:17141–17149 (1990).

Send reprint requests to: Dr. J. P. Glusker, The Institute for Cancer Research, The Fox Chase Cancer Center, Philadelphia, PA 19111.